Chemical Physics Letters 645 (2016) 157–163

Contents lists available at ScienceDirect

Chemical Physics Letters

journal homepage: www.elsevier.com/locate/cplett

New findings on the influence of carbon surface curvature on energetics of benzene adsorption from gaseous phase

Artur P. Terzyk[a], Sylwester Furmaniak[a], Marek Wiśniewski[a,b,*], Karolina Werengowska[a], Piotr A. Gauden[a], Piotr Kowalczyk[c]

[a] Faculty of Chemistry, Physicochemistry of Carbon Materials Research Group, Nicolaus Copernicus University in Toruń, ul. Gagarina 7, 87-100 Toruń, Poland
[b] INVEST-TECH R&D Center, ul. Plaska 32-34, 87-100 Toruń, Poland
[c] School of Engineering and Information Technology, Murdoch University, Murdoch, WA 6150, Australia

ARTICLE INFO

Article history:
Received 5 October 2015
In final form 23 December 2015
Available online 30 December 2015

ABSTRACT

In this Letter, new results of calorimetric study on benzene adsorption from the gaseous phase are presented. According to some of recently published reports, the energy of solid–fluid, interactions increases with the rise in carbon nanotube curvature during adsorption. The recent considerations [Chem. Phys. Lett. 619 (2015) 219] on thermodynamics of adsorption from aqueous solutions on a series of carbon nanotubes have confirmed this observation. Although comparable 'energy–tube diameter' relations for benzene adsorption from the solution and from the gaseous phase are observed, remarkable differences between the mechanisms of the both processes caused by surface heterogeneity are noticeable.

1. Introduction

It is commonly known that energy of van der Waals interactions between adsorbed molecules and external walls of tubes should decrease together with the rise in curvature of carbon nanotubes (CNTs). This should be visible especially in the case of 'flat' and 'rigid' molecules, since the distance between surface atoms and interacting centres located on molecules increases with the rise in surface curvature. In order to explain some nuances about of benzene/nanotube system, the results of theoretical calculations can be used. Tournus and Charlier [1] studied the interaction between benzene molecules and carbon nanotubes using ab initio calculations.

In general, the results presented by the above mentioned authors show that, in the case of tubes with small radii, the 'bridge' position with the benzene molecule situated over a C—C bond is most favourable. Generally, except for small armchair tubes, the nanotubes investigated by those authors tend to present decreasing reactivity simultaneously with curvature. However, as it was emphasised by the authors, the calculations were performed for specific conditions which are not always relevant to experiments performed on real nanotubes. First of all, 'perfect' nanotubes i.e. with neither defects nor impurities, were considered. It was assumed that localised adsorption cannot occur at room temperature.

In fact, the ab initio calculation results show that benzene molecules adsorbed on nanotubes can easily slide on a C—C bond, and the energy of benzene rotation around the axis passing through its centre and normal to the nanotube surface is not large. Thus, low temperature is necessary to observe localised adsorption.

From the study by Tournus and Charlier [1], certain interesting conclusions can be drown. They are comparable to the results obtained recently [2,3]. Namely, it is claimed that the curvature effect manifests itself with the general trend of a higher reactivity for smaller tube diameters, i.e. it was confirmed by introducing the concept of the π orbital axis vector – POAV. The situation observed for 'bridge' benzene configuration is the exception in which the energy of benzene-nanotube interaction increases i.e. becomes more negative with the rise in the tube curvature (see Fig. 3 in [1]). The results indicate that *s–p* mixing of π electrons increases together with curvature, so the π orbital directionality is enhanced, which results in higher overlapping with the wave functions of adsorbed benzene molecules.

Some experimental data have recently been published confirming these considerations [3–6]. It was indicated, that together with the rise in carbon nanotubes curvature, the energy of solid–fluid interactions increases. Pioneering papers by Castillejos et al. [3], Hilding et al. [4], and Menon et al. [5] involve experimental evidence of this effect. Komarneni et al. [6], on the basis of

* Corresponding author at: Physicochemistry of Carbon Materials Research Group, Faculty of Chemistry, Nicolaus Copernicus University, ul. Gagarina 7, 87-100 Toruń, Poland.
E-mail address: Marek.Wisniewski@umk.pl (M. Wiśniewski).

http://dx.doi.org/10.1016/j.cplett.2015.12.052
0009-2614/

the thermal desorption spectroscopy study, calculated the values of benzene binding energies on carbon nanotubes of diameters between 0.7 and 1.4 nm. The obtained values ranged between 36.8 and 46.3 kJ/mol for adsorption on the external sites and grooves. The energy of adsorption on the HOPG surface was equal to 43.7 kJ/mol.

GCMC simulation results obtained by Vernov and Steele [7] show that the solid–fluid potential energy of interaction between benzene and graphite is equal to ca. 38.6 kJ/mol (see Fig. 6). This value corresponds well to the enthalpy of adsorption determined calorimetrically by Pierotti and Smallwood (38.6 kJ/mol) [8,9] and by Isirikyan and Kiselev (40.5 kJ/mol) [10]. The value of binding energy obtained by Komarneni et al. [6] for benzene on HOPG (43.7 kJ/mol) is similar to the value determined calorimetrically, especially by Isirikyan and Kiselev [10]. The differences between simulation, calorimetry, and TDS can be caused by differences in the surface nature of perfect infinitive graphite (simulation), graphitised carbon blacks (calorimetry) and HOPG (TDS). Also, the procedure applied during the calculation of binding energy from the TDS peak, i.e. Redhead equation and a standard pre-exponential factor of 1×10^{13}/s, is approximate. Moreover, since the energy of solid–fluid interactions is almost equal to the enthalpy of adsorption at very small coverages, assuming that the potential energy of the solid–fluid interaction is remarkably larger than the energy of translational degrees of freedom lost by adsorbed molecules, some molecules can be adsorbed on defected sites. Thus, the calorimetrically measured enthalpy can be determined with error. Additionally, Komarneni et al. [6] concluded that the results are in a qualitative agreement with the DFT calculation predicting only a very small increase in the binding energies with an increasing nanotube diameter.

The report [2] on the energetics of benzene adsorption from aqueous solutions on carbon nanotubes of different diameter, has provided some experimental correlations showing that, together with the rise in curvature of nanotubes, the energy of benzene-tube wall interactions (adsorption on external surface) increases. It was also concluded that the most probable effect causing this rise in energy is the change in carbon hybridisation with the change in curvature, i.e. sp^3 carbon atoms forming pore walls are more reactive than the sp^2 ones.

In our previous study [2] it was concluded that it would be desirable to check the energetics of benzene adsorption from the gaseous phase for the same series of nanotubes. Thus, in the present Letter some new calorimetric results of benzene adsorption from gaseous phase on two series of nanotubes having different diameters are reported. The calorimetric results of benzene adsorption on nanotubes studied herein have not been published yet. The obtained results are analysed using a recently developed new adsorption isotherm model.

2. Experimental methods

Seven commercially available, high purity, closed carbon nanotubes (purchased from Nanostructured & Multi-Walled Amorphous Materials (Nanoamor, Houston, TX, USA) and Helix Material Solutions (Richardson, TX, USA)) are investigated.

The A series tubes from Nanoamor were single-walled (labelled A-0) as well as multi-walled carbon nanotubes (labelled as A-1, A-2, and A-3, and were described previously [2,11,12]). The second series from Helix (labelled H) contains single-walled (H-1), double-walled (H-2), and multi-walled carbon nanotubes (H-3) [2,11,12].

High-resolution transmission electron microscopy (HRTEM) images were taken using a transmission electron microscope F20X-TWIN (FEI-Tecnai) operating at 200 kV [11,13]. Previous HRTEM studies [11,13] of the H series revealed that the sample of the so-called single walled nanotubes (H-1) seems to contain no single-walled tubes. It contains multi-walled tubes. The so-called double walled tube sample (labelled H-2) actually contains some double-walled tubes, but tubes with three or more layers are prevalent. Some new HRTEM pictures are collected in Figure S1 in the Supplementary Data section.

Table 1
Characteristics of carbon nanotubes studied: diameter (D_{exp}), the number of walls ($n_{w,exp}$) and the BET surface area (S_{BET}) calculated from low-temperature nitrogen adsorption data [2,11,12].

Nanotube	D_{exp} [nm]	$n_{w,exp}$	S_{BET} [m^2/g]
A-0	1–2[a] (2[b])	1–2[a] (1[b])	1170
A-1	<8[a] (6[b])	4–7[a] (6[b])	449
A-2	8–15[a] (11[b])	10–14[a] (12[b])	294
A-3	10–30[a] (20[b])	18–30[a] (24[b])	112
H-1	~1.3[a] (7.7[b])	2–4[a] (3[b])	365
H-2	4[a] (4[b])	2–5[a] (4[b])	602
H-3	<10[a] (10[b])	10–20[a] (15[b])	298

[a] Data provided by the producer.
[b] Maximum values for the distribution of diameters.

In order to characterise the structure of the nanomaterials studied, N_2 adsorption–desorption isotherms at 77 K were measured using the ASAP 2010 (Micromeritics) sorption apparatus. From the obtained data, the BET surface area values were calculated. The detailed structural characteristics are collected in Table 1.

Benzene adsorption isotherms were measured volumetrically (T = 298 K), and the differential adsorption enthalpy (q^{diff}) was determined with a Tian-Calvet isothermal microcalorimeter (for details, see e.g. [14]).

3. Theoretical model applied for description of experimental data

From all the theoretical models able to describe the II (and III) type of adsorption isotherm (according to the IUPAC classification) suggested, the generalised D'Arcy and Watt equation (GDW) [15] is one of those most advanced. This approach assumes a two-step mechanism of the process. The adsorption of molecules on primary adsorption sites of the adsorbent surface is the first step. Such molecules become the secondary adsorption centres allowing multilayer adsorption. Although the GDW equation was initially derived to describe water adsorption on carbonaceous materials [15], this equation (and/or its modifications) has also been successfully used to fit adsorption isotherms of different gases on different materials [15–17], also on CNTs [14]. One of the original GDW equation modifications is the multi-site GDW model (MSGDW) [15]. It is well-documented that the surface defects are present on the nanotubes walls [18,19]. Thus, the presence of defects should be taken into account in theoretical approach. The existence of different kinds of primary centres is also assumed in our model. They may differ in the value of adsorption energy and/or equilibrium binding constants. Due to this assumption, it is possible to generate various shapes of adsorption enthalpy, similar to the experimentally observed ones [15]. Hence, in this study, the MSGDW model was used to analyse experimental data of benzene adsorption on CNTs. In the model, the presence of three types of primary adsorption sites was assumed. This is the smallest number necessary to generate different shapes of adsorption enthalpy including non-monotonic ones [15]. Moreover, the assumption that a larger number of primary site types are present does not remarkably change the quality of the fit. Thus, the MSGDW adsorption isotherm equation may be written in the form:

$$a = \left(\sum_{i=1}^{3} \frac{a_{m,i} K_{L,i} h}{1 + K_{L,i} h} \right) \times \left(1 + \frac{cwh}{1 - ch} \right) \quad (1)$$

where $a_{m,i}$ denotes the surface concentration of the ith kind of primary sites, $K_{L,i}$ and c are the equilibrium constants related to the adsorption on the ith type of primary and on secondary centres, respectively; w is the parameter that determines which part of benzene molecules adsorbed on all the kinds of primary centres converts into the secondary ones, and h is the relative pressure, i.e. the ratio of equilibrium and saturation C_6H_6 vapour pressure at the given temperature.

It is assumed that $a_{m,i}$ and w parameters are temperature-independent, while the equilibrium constants decrease with the rise in T according to the basic thermodynamic formulas (for details see [15] and references therein):

$$K_{L,i} = K^0_{L,i} \exp\left[-\frac{Q_{\mathrm{prim},i} - L}{\mathrm{RT}}\right] \tag{2}$$

$$c = c^0 \exp\left[-\frac{Q_{\mathrm{sec}} - L}{\mathrm{RT}}\right] \tag{3}$$

where $K^0_{L,i}$ and c^0 are almost temperature-independent, pre-exponential factors, $Q_{\mathrm{prim},i}$ and Q_{sec} are the adsorption enthalpy values on the ith kind of primary sites and on secondary ones, respectively; L is the benzene condensation enthalpy and R is the universal gas constant. On the basis of the isosteric adsorption enthalpy definition [15]:

$$q^{\mathrm{st}} - L = -\mathrm{RT}^2\left(\frac{\partial \ln h}{\partial T}\right)_a \tag{4}$$

and with the use of differential calculus combining Eqs. (1)–(3), the following formula can obtained:

$$q^{\mathrm{st}} = \frac{\left(\sum_{i=1}^{3} \frac{a_{m,i}K_{L,i}}{(1+K_{L,i}h)^2} \times Q_{\mathrm{prim},i}\right) \times \left(1 + \frac{cwh}{1-ch}\right) + \left(\sum_{i=1}^{3} \frac{a_{m,i}K_{L,i}h}{1+K_{L,i}h}\right) \times \frac{cw}{(1-ch)^2} \times Q_{\mathrm{sec}}}{\left(\sum_{i=1}^{3} \frac{a_{m,i}K_{L,i}}{(1+K_{L,i}h)^2}\right) \times \left(1 + \frac{cwh}{1-ch}\right) + \left(\sum_{i=1}^{3} \frac{a_{m,i}K_{L,i}h}{1+K_{L,i}h}\right) \times \frac{cw}{(1-ch)^2}} \tag{5}$$

The isosteric adsorption enthalpy is related to the differential one according to the well known relation [20]:

$$q^{\mathrm{diff}} = q^{\mathrm{st}} - \mathrm{RT} \tag{6}$$

The MSGDW model (Eqs. (1) and (5)) is used to simultaneously describe the experimental benzene adsorption isotherms and the related differential adsorption enthalpy on all the considered nanotube samples. The fitting is performed with the genetic algorithm proposed by Storn and Price [21]. The goodness of both the isotherm and enthalpy fits are estimated using the determination coefficients:

$$\mathrm{DC}_a = 1 - \eta_a \tag{7}$$

$$\mathrm{DC}_q = 1 - \eta_q \tag{8}$$

where

$$\eta_a = \frac{\sum_{i=1}^{NP_a}(a_{\mathrm{exp},i} - a_{\mathrm{theo},i})^2}{\sum_{i=1}^{NP_a}(a_{\mathrm{exp},i} - \bar{a}_{\mathrm{exp}})^2} \tag{9}$$

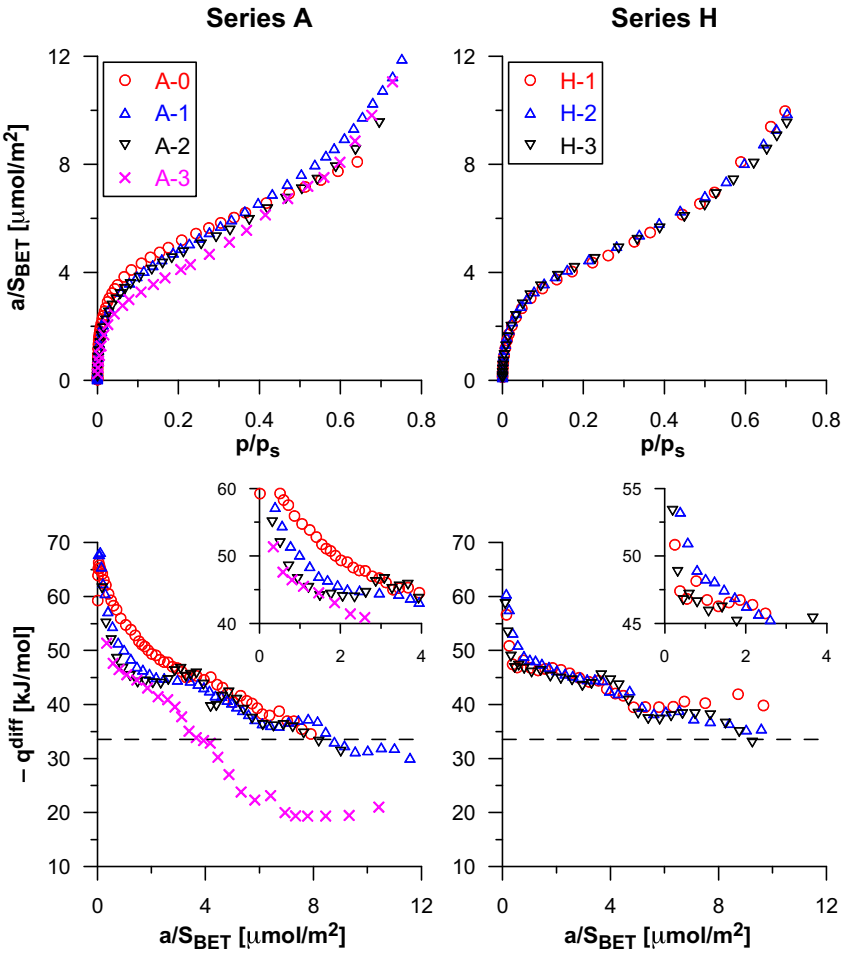

Figure 1. The comparison of benzene adsorption isotherms (T = 298 K) and related differential enthalpy of adsorption for all the considered nanotubes. The dashed lines on lower panels represent the enthalpy of benzene condensation.

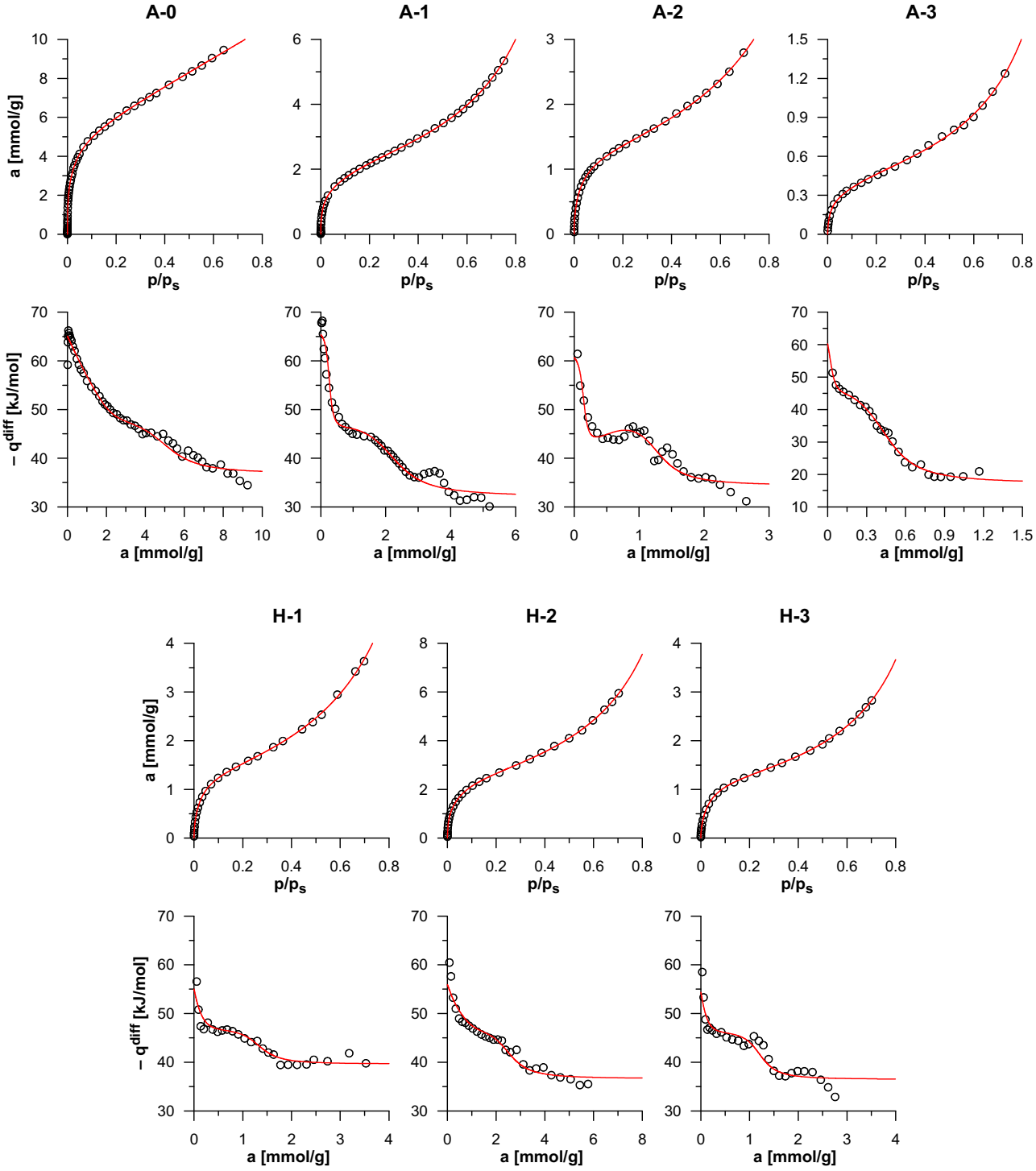

Figure 2. Graphical representations of the experimental data (C_6H_6 adsorption isotherms and related enthalpy) fitting by the MSGDW model (Eqs. (1) and (5)). Points – experimental data, lines – theoretical model.

$$\eta_q = \frac{\sum_{i=1}^{NP_q}\left(q^{\mathrm{diff}}_{\mathrm{exp},i} - q^{\mathrm{diff}}_{\mathrm{theo},i}\right)^2}{\sum_{i=1}^{NP_q}\left(q^{\mathrm{diff}}_{\mathrm{exp},i} - \bar{q}^{\mathrm{diff}}_{\mathrm{theo}}\right)^2} \tag{10}$$

where NP_a and NP_q are the number of points on the curves, subscripts 'exp' and 'theo' indicate the experimental and theoretical values for the ith point, respectively; and $\bar{x}_{\mathrm{exp}}$ is the average experimental value of x. The global minimising parameter representing the goodness of both the adsorption and the enthalpy fitting is defined as (geometric mean):

$$\mathrm{DC} = 1 - \sqrt{\eta_a \times \eta_q} \tag{11}$$

4. Results and discussion

4.1. Adsorption from gas phase

In Figure 1, the comparison of benzene adsorption isotherms and calorimetrically measured differential adsorption enthalpy, for all

Table 2
The values of the best-fit parameters obtained from MSGDW model (Eqs. (1) and (5)) for the simultaneous description of benzene adsorption isotherms and related differential enthalpy of adsorption for all the considered nanotubes.

Nanotubes	$a_{m,i}$[a] [mmol/g]	$K_{L,i}$[a]	w	c	$Q_{prim,i}$[a] [kJ/mol]	Q_{sec} [kJ/mol]	DC_{iz}	DC_q
A-0	0.6714	1360	26.85	0.04764	−91.44	−34.26	0.9997	0.9814
	1.307	754.4			−37.54			
	3.255	28.91			−45.26			
A-1	0.2702	7491	0.6876	0.8684	−63.95	−29.50	1.0000	0.9750
	0.8703	119.8			−43.69			
	1.461	6.037			−44.17			
A-2	0.1507	5839	0.9887	0.7791	−59.37	−31.79	0.9999	0.9372
	0.4043	111.6			−38.46			
	0.7940	17.09			−46.22			
A-3	0.03148	1712	0.7895	0.9090	−64.59	−14.42	0.9993	0.9925
	0.2103	104.6			−42.33			
	0.3092	5.359			−40.71			
H-1	0.05662	1622	1.099	0.8732	−66.54	−37.08	0.9997	0.9707
	0.2130	570.6			−44.33			
	1.134	30.05			−44.15			
H-2	0.2003	1194	0.8353	0.8753	−60.39	−34.07	0.9999	0.9849
	0.6112	334.7			−46.80			
	1.880	16.88			−44.07			
H-3	0.05606	1726	0.7614	0.9047	−60.14	−33.94	0.9999	0.9421
	0.1533	493.0			−44.35			
	1.065	25.74			−43.62			

[a] The values of parameters connected with different kinds of primary adsorption sites are ordered according to the decreasing value of Langmuir constants.

the studied systems are presented. As can observed for the A series, the differences between isotherms as well as adsorption enthalpy are strongly pronounced. In contrast, for the H series, they are small. However, for the both series, a similar tendency can be observed, i.e. the differential adsorption enthalpy at low coverage decreasing with the rise in the diameter of a nanotube. Obviously, at low coverages, the solid–fluid interaction energy predominates, and this energy has the major contribution to the differential adsorption enthalpy. In order to observe the correlations between the enthalpy and diameters of nanotubes, the data presented in Figure 1 were described with the use of the above-mentioned MSGDW model (Eqs. (1), (5), as well as (6)), and the simultaneous isotherm and enthalpy fitting procedure (Eqs. (7)–(11)).

As can be seen from the analysis of the data collected in Figure 2, the proposed MSGDW adsorption isotherm equation (and the corresponding enthalpy formula) satisfactorily describes the experimental data (the best-fit parameters values are collected in Table 2). What should also be emphasised, some nuances appearing on the enthalpy plots are very well recovered by the model. It is however worth noticing that, for all the studied nanotubes, the energy of interaction with the 'primary' sites ($Q_{prim,i}$ – see Table 2) is remarkably higher than the energy of interaction with the secondary ones (Q_{sec}).

Since the presence of three types of primary adsorption sites is assumed in our model (Eq. (1)), the energy of solid–fluid interactions should be calculated as the weighed average with the use of the results collected in Table 2 and the following equation:

$$Q_{prim,av} = \frac{\sum_{i=1}^{3} a_{m,i} \times Q_{prim,i}}{\sum_{i=1}^{3} a_{m,i}} \quad (12)$$

The total solid–fluid interactions energy in monolayer per mass unit of nanotubes was additionally calculated using:

$$\Delta H_m = \sum_{i=1}^{3} a_{m,i} \times Q_{prim,i} \quad (13)$$

The results are plotted in Figure 3 and collected in Table S1 in Supplementary Data. For all the nanotubes, the linear/hyperbolic-like correlation between the average/total energy of solid–fluid interactions and nanotube diameters can be noticed. It should also be pointed that the values of $Q_{prim,av}$ are, with one exception, larger than the binding energy values observed for HOPG surface (see Table S1 in Supplementary Data [6]). The observed benzene binding energy values are higher than those calculated from DFT and reported in [1]. Komarneni et al. [6] have recently discussed some additional problems connected with the DFT calculations. These calculations can be the treatment of long range (dispersion) interactions and some limitations in the choice of the appropriate basis sets to expand the Kohn–Sham orbitals as well as the size of the unit cell used. The authors [6] pointed out that, due to the limitations mentioned as well as some additional approximations, the binding energy values calculated from DFT are often underestimated.

4.2. Adsorption from solution vs. adsorption from gas phase

In this Letter, a correlations similar to that reported in Figure 3 were described for the same nanotubes and for benzene adsorption enthalpy data measured for adsorption from aqueous solutions [2] i.e. the correlation between the integral benzene adsorption enthalpy and D_{exp}, see Fig. 1 in [2]). It indicates the fact that, during adsorption from the solution, taking into account the presence of different types of adsorption centres on nanotube surface, as it was done for gas adsorption data, was unnecessary. For adsorption from the gaseous phase, the correlations reported in Figure 3 are observed only if the heterogeneity of adsorption sites is taken into consideration (see Eq. (1)). The correlation between the total concentration of the active sites calculated from the MSGDW model and the BET surface area of the studied nanotubes obtained from low-temperature N_2 adsorption data (and shown in Figure 4a) confirms that for benzene at 298 K and for nitrogen at 77 K the same surface active centres are accessible. In contrast, during adsorption from the solution, as it was shown with MD simulation technique, benzene molecules form patches on the surface of nanotubes, and no creation of the typical monolayer was observed [22]. Water

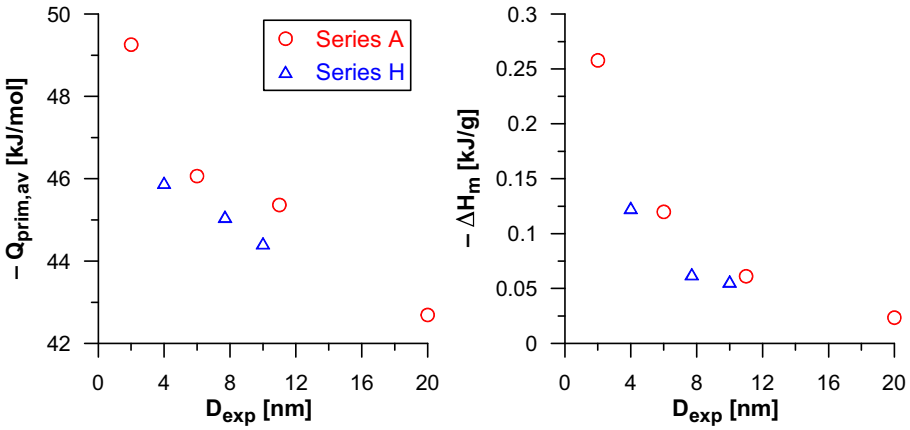

Figure 3. The correlation between average energy of adsorption on primary sites ($Q_{prim,av}$, Eq. (12)) or the total energy of interaction of molecules binding in monolayer (ΔH_m, Eq. (13)) and the diameter of nanotubes.

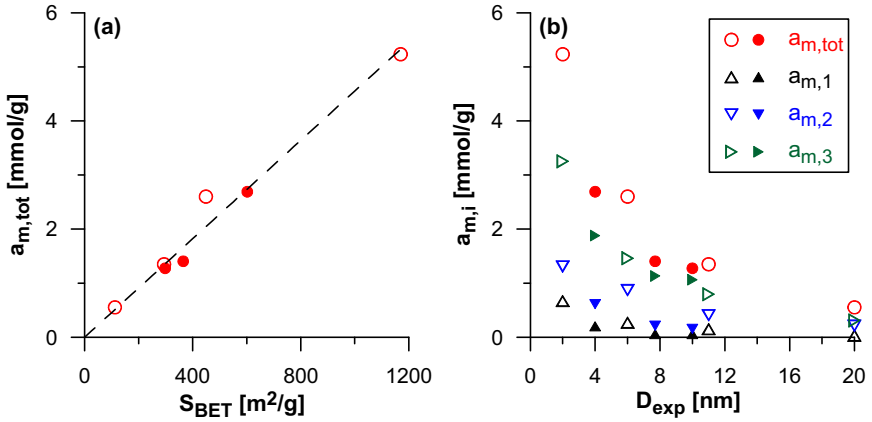

Figure 4. (a) Correlation between total concentration of primary sites calculated from the MSGDW model ($a_{m,tot} = \sum_{i=1}^{3} a_{m,i}$) and the BET surface area (open and full symbols are related to the A and H series, respectively; the dashed line is drawn to guide the eye). (b) The concentration of different kinds of primary sites (and their total concentration) plotted as the function of nanotube diameters.

is adsorbed between those patches covered by adsorbed benzene molecules. It could be concluded that the surface heterogeneity of the studied systems is more pronounced for adsorption from the gaseous phase rather than for adsorption from the solution.

4.3. Role of heterogeneity in adsorption from gas phase

To sum up, it is worth noticing that, for studied nanotubes, during benzene adsorption, essentially the same correlation between energy and the tube diameter is observed. In order to explain the role of heterogeneity in Figure 4b, the correlations between the concentrations of primary active sites calculated from MSGDW model and tube diameters are collected. As can be seen above, the decrease in the tube diameter leads to the creation of all three types of centres. For all the tubes, the largest concentration is observed for the centres in which the smallest energy of solid–fluid interactions (around 45 kJ/mol) is involved. The two remaining types of centres for larger nanotubes exhibit similar concentrations and the differences are visible only for the smallest tubes studied. This finally leads to the hyperbolic-type relationship between the total concentration of active sites and D_{exp} (Figure 4b).

5. Summary

Reassuming, for both, the adsorption from a solution and the adsorption from the gaseous phase, the same relation between energy and the tube diameters is observed. The surface heterogeneity in adsorption from the gaseous phase leading to the appearance of correlations reported in Figures 3 and 4 needs further theoretical and experimental studies, and the results will be reported in the near future.

Finally, it was shown here that, for adsorption from the gaseous phase, a similar influence of curvature on energetic of adsorption as during adsorption from the aqueous solution is observed. However, during adsorption from the gaseous phase surface, heterogeneity of tube walls is manifested more strongly than during adsorption from the solution.

Appendix A. Supplementary data

Supplementary data associated with this article can be found, in the online version, at doi:10.1016/j.cplett.2015.12.052.

References

[1] F. Tournus, J.-C. Charlier, Phys. Rev. B 71 (2005) 165421.
[2] M. Wiśniewski, K. Werengowska-Ciećwierz, A.P. Terzyk, Chem. Phys. Lett. 619 (2015) 219.
[3] E. Castillejos, B. Bachiller-Baeza, I. Rodríguez-Ramos, A. Guerrero-Ruiz, Carbon 50 (2012) 2731.
[4] J. Hilding, E.A. Grulke, S.B. Sinnott, D. Qian, R. Andrews, M. Jagtoyen, Langmuir 17 (2001) 7540.
[5] M. Menon, A.N. Andriotis, G.E. Froudakis, Chem. Phys. Lett. 320 (2000) 425.

[6] M. Komarneni, A. Sand, J. Goering, U. Burghaus, M. Lu, L.M. Veca, Y.-P. Sun, Chem. Phys. Lett. 476 (2009) 227.
[7] A. Vernov, W.A. Steele, Langmuir 7 (1991) 2817.
[8] R.A. Pierotti, R.E. Smallwood, J. Colloid Interface Sci. 22 (1966) 469.
[9] R.A. Pierotti, Chem. Phys. Lett. 2 (1968) 420.
[10] A.A. Isirikyan, A.V. Kiselev, J. Phys. Chem. 65 (1961) 601.
[11] M. Wiśniewski, P.A. Gauden, A.P. Terzyk, P. Kowalczyk, A. Pacholczyk, S. Furmaniak, J. Colloid Interface Sci. 391 (2013) 74.
[12] A. Pacholczyk, A.P. Terzyk, M. Wiśniewski, P.A. Gauden, R.P. Wesołowski, S. Furmaniak, A. Szcześ, E. Chibowski, B. Kruszka, J. Colloid Interface Sci. 361 (2011) 288.
[13] S. Furmaniak, A.P. Terzyk, P.A. Gauden, P.J.F. Harris, M. Wiśniewski, P. Kowalczyk, Adsorption 16 (2010) 197.
[14] S. Furmaniak, A.P. Terzyk, G. Rychlicki, M. Wiśniewski, P.A. Gauden, P. Kowalczyk, K.M. Werengowska, K. Dulska, J. Colloid Interface Sci. 349 (2010) 321.
[15] S. Furmaniak, P.A. Gauden, A.P. Terzyk, G. Rychlicki, Adv. Colloid Interface Sci. 137 (2008) 82.
[16] S. Furmaniak, A.P. Terzyk, R. Gołembiewski, P.A. Gauden, L. Czepirski, Food Res. Int. 42 (2009) 1203.
[17] S. Furmaniak, Transp. Porous Media 92 (2012) 21.
[18] D.B. Mawhinney, V. Naumenko, A. Kuznetsova, J.T. Yates Jr., J. Liu, R.E. Smalley, Chem. Phys. Lett. 324 (2000) 213.
[19] P. Kondratyuk, J.T. Yates Jr., Acc. Chem. Res. 40 (2007) 995.
[20] S. Ross, J.P. Olivier, On Physical Adsorption, John Wiley & Sons, Inc., New York, 1964.
[21] R. Storn, K. Price, J. Glob. Optim. 11 (1997) 341.
[22] A.P. Terzyk, P.A. Gauden, S. Furmaniak, R.P. Wesołowski, P.J.F. Harris, P. Kowalczyk, Phys. Chem. Chem. Phys. 11 (2009) 9341.